Available online at www.sciencedirect.com
ScienceDirect
Carbohydrate Research 343 (2008) 2172–2183
Carbohydrate RESEARCH

MALDI-QTOFMS/MS identification of glycoforms from the urine of a CDG patient

Sergey Y. Vakhrushev,[a] Marten F. Snel,[b] James Langridge[b] and Jasna Peter-Katalinić[a,*]

[a]*Institute for Medical Physics and Biophysics, Biomedical Analysis, University of Muenster, D-48149 Muenster, Germany*
[b]*Waters Corporation, Atlas Park, Simonsway, Manchester M22 5PP, UK*

Received 21 September 2007; received in revised form 9 November 2007; accepted 12 November 2007
Available online 22 November 2007

Presented at Eurocarb 14th Lübeck, Germany, September 2007

Abstract—Identification of single glycoconjugate components in a complex mixture from the urine of a patient suffering from a congenital disorder of glycosylation was probed by MALDIMS analysis on a hybrid quadrupole time-of-flight instrument. In negative ion mode, complex maps containing more than 50 ionic species were obtained and a number of molecular ions directly assigned using a previously developed computer-assisted algorithm. To confirm the data and determine the carbohydrate sequence, single molecular ions were selected and submitted to fragmentation experiments. Interpretation of fragmentation spectra was also assisted by the software using alignment with spectra generated in silico. According to fragmentation data, the majority of glycoconjugate ionic species could be assigned to free oligosaccharides along with ten species tentatively assigned to glycopeptides. Following this approach for glycan identification by a combination of MALDI-QTOFMS and MS/MS experiments, computer-assisted assignment and fragment analysis, data for a potential glycan data base are produced. Of high benefit for this approach are two main factors: low sample consumption due to the high sensitivity of ion formation, and generation of only singly charged species in MALDIMS allowing interpretation without any deconvolution. In this experimental set-up, sequencing of single components from the MALDI maps by low energy CID followed by computer-assisted assignment and data base search is proposed as a most efficient strategy for the rapid identification of complex carbohy-drate structures in clinical glycomics.

Keywords: Glycomics; Glycoconjugates; MALDI-QTOFMS; Congenital disorders of glycosylation; Computer-assisted calculations

1. Introduction

Structural and functional analysis of glycosylation in human urine has been established to monitor changes in glycosylation status in healthy persons and diseased patients and to indicate possible aberrant structures as possible biomarkers for congenital diseases. The analytical task to carry such investigation is to establish analytical strategies which include as complete as possible structural identification of any glycoforms present. Among a number of strategies for the structural analysis of glycoconjugates in pre-separated fractions or in complex mixtures obtained from native sources, mass spectrometry represents one of the most efficient methods for mapping and sequencing at high sensitivity and accuracy of identification.[1–6]

Congenital disorders of glycosylation (CDG) are defined as inherited metabolic diseases caused by low or missing activity of enzymes, transporters or other functional proteins responsible for glycosylation processing pathways of glycoconjugates.[7,8] The observation of the decreased serum thyroxin-binding globulin and increased arylsulfatase A activity in two patients with familial psychomotor retardation reported by Jaeken et al.[9] was the basis of the CDG discovery. In 1984, Jaeken et al.[10] determined sialic acid deficiency in serum and cerebrospinal fluid transferrin from identical twin sisters suffering from demyelinating disease. That was the first demonstration of a new syndrome caused by defective

* Corresponding author. Tel.: +49 251 83 52308; e-mail: jkp@uni-muenster.de

0008-6215/$ - see front matter © 2007 Elsevier Ltd. All rights reserved.
doi:10.1016/j.carres.2007.11.014

protein glycosylation. To date most of the presently known CDG cases are related to abnormalities in the N-glycosylation pathway of glycoproteins with only few O-glycosylation diseases identified.[11] CDGs belong to rare diseases: around 500 cases of all types of CDG have been discovered so far.[12] The types of CDG diseases have been classified into two main groups, according to the glycosylation pathway damage.[13]

Presently, serum transferrin IEF is the most widely used method for CDG diagnosis. Our attention, however, was turned towards glycopatterns in urine as an alternative source of glycoconjugate biomarkers and therefore potentially useful diagnostic tool to be correlated with a clinical picture of human disorders.[14–21]

In comparison to the healthy control, the urine of CDG patients was shown to contain O-linked glycans and glycosylated amino acids at concentrations two-to-three orders of magnitude higher.[17] In urine analysis of CDG patients by MS, we applied several approaches such as high resolution/high-mass accuracy FT-ICR MS,[18] capillary-based[19] and chip-based nano-ESI-QTOF CID fragmentation analysis,[20] where we were able to identify from 40% to 75% of components using manual and computer-assisted data interpretation strategy. However, it is known that in ionization process due to still largely unknown factors, different components express different ionization properties, which causes an incomplete overlap of in-toto detected components.[22] In this study, a MALDI mapping by MS and sequencing by MS/MS for high coverage of glycoform identification in the urine of a CDG patient using the QTOF mass analyzer is presented, involving high sensitivity and low sample consumption. An additional helpful feature of the MALDI ionization is the production of predominantly singly charged ionic species, which do not require deconvolution, generating simpler spectra and enhancing data interpretation.

MS fragmentation of complex glycans was already introduced to analytical glycobiology 20 years ago,[23] but an assignment of a carbohydrate structure from a single experiment still represents a challenging task. Basic structural predictions can be proposed for diverse N- and O-glycan involving already known biosynthetic pathways, such as N-glycans which include variations of the common $Man_3GlcNAc_2$ pentasaccharide core, or O-glycans of the GalNAc core type.[24] A number of techniques has been applied for the structural elucidation of components in carbohydrate mixtures, basically attempting to find diagnostic fragment ions responsible for single structures.[25–35] Five series of fragment ions are generally expected: the most prone to occur is the cleavage of one glycosidic bond, resulting in two types of fragments with the reducing or the non-reducing end.[36] Additional cleavage of a second glycosidic bond might result into the third series, called internal fragments. The last two series are produced by the double cleavage of the glycosidic ring (cross-ring) and contain either the reducing or the non-reducing end of the precursor ion. The combinations between these series, such as triple glycosidic or glycosidic and cross-ring dissociation have often been observed.[1,3,14,18–20,28–30,35,37] The first three series represent major tools for structural elucidation, while according to the cross-ring fragmentation linkage branching patterns can be established. Distinct fragmentation patterns under controlled collision energy and gas conditions along with the ability of automatic switching between MS and MS/MS mode by electrospray (ESI) QTOF instrument represent a powerful option for high-throughput analysis of complex carbohydrate mixtures. Cleavage ions obtained by tandem mass spectrometry are described according to the fragmentation nomenclature introduced by Domon and Costello (Fig. 1).[38]

Letters A_i, B_i, C_i are used for the assignment of the fragmentation with the charge at the non-reducing end, where index '*i*' determines the number of the glycosidic bond calculated from the non-reducing side. Those fragmentations, which carry the charge at the reducing end, have been denoted as X_j, Y_j and Z_j, counting the order number from that side. Cross-ring fragmentation has been denoted by letters A_i and X_j, where the exact position of the sugar ring cleavages is determined by superscript at

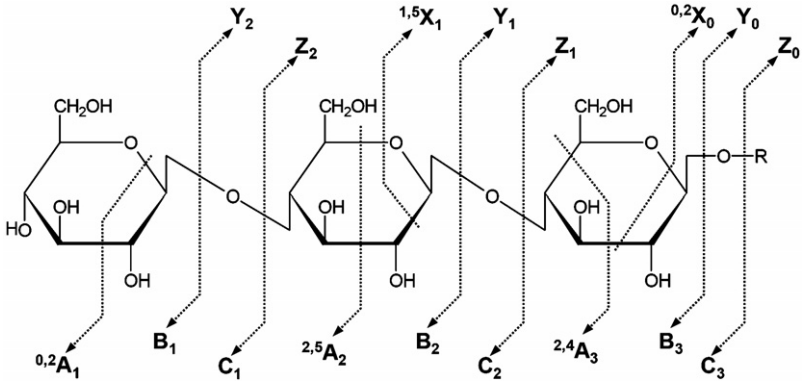

Figure 1. Nomenclature of oligosaccharide fragmentation pattern introduced by Domon and Costello.[38]

the upper left side. In the case of branched structures Greek symbols (α, β, γ) have been introduced as subscript at the right side to distinguish between fragments originating from different antennae, where α represents the largest one. Thus, β, γ are assigned with decreasing molecular (fragment) mass ($\alpha \geqslant \beta \geqslant \gamma$). Further branching of the 'primary' antennae has been proposed to be named α′, β′, γ′ and α″, β″, γ″, where $\alpha' \geqslant \alpha''$, $\beta' \geqslant \beta''$, etc.[35,38]

2. Experimental

2.1. Reagents and samples

Methanol was obtained from E. Merck (Darmstadt, Germany) and used without further purification. Distilled and deionized water (Mili-Q water systems Millipore, Bedford, MA, USA) was used for the preparation of the sample solutions. 2,4,6-Trihydroxyacetophenone (THAP) and diammonium citrate (DAC) were purchased from Sigma (Taufkirchen, Germany). The sample investigated in this study was a native glycoconjugate mixture, from the urine of patient A.L., suffering from symptoms of CDG. For isolation of components, the patient's urine was filtered and submitted to a first gel filtration chromatography on Biogel P2 as described before.[17–19] The fraction B2 was further submitted to a second gel filtration chromatography performed on Fractogel TSK HW 50 with 0.01 M pyridinium acetate at pH 5.4 as the eluting buffer and the fraction F2 thereof to the anion-exchange chromatography on MonoQ to deliver 6 fractions, from which the fraction M3 was used in the present study.

2.2. Matrix preparation

MALDI matrix used in the present study for the analysis of oligosaccharides and glycoconjugates was prepared as follows: 1 mg of THAP was dissolved in 1:1 EtOH–aq DAC 20 mM (1 mL).

2.3. MALDI target spots preparation

MALDI target spots were prepared by the "thin layer" method. The matrix soln (0.5 μL) was loaded onto the target and dried under a gentle stream of air or nitrogen. Afterwards, 0.5 μL of the sample soln was deposited on the matrix layer and immediately dried with a gentle stream of air or nitrogen. The final sample amount on each spot was approximately 1–2 pmol as derived from the dried sample weight taking into account an average molecular mass of 1200 Da for the glycoconjugate species present.

2.4. MALDI-QTOFMS and CID MS/MS

Mass spectrometry was performed on a MALDI-QTOF Premier mass spectrometer (Waters, Manchester, UK) fitted with a 200 Hz repetition rate neodymium:yttrium-aluminium-garnet laser ($\lambda = 355$ nm). The mass spectrometer was operated in negative ion mode and prior to analysis was calibrated over the m/z range 50–3000 using dextran from *Leuconostoc mesenteroides* (Sigma, Gillingham, UK).

Mass spectra were acquired manually over the m/z range 800–3000. The peptide standard, [Glu^1]-fibrinopeptide (Sigma, Gillingham, UK), was spotted on the MALDI target plate at a concentration of 50 fmol on target, on lock mass target-positions, adjacent to the samples under investigation. Following MS acquisition from the glycoconjugates sample, the peptide standard was used to provide accurate mass data.

In MS/MS mode, precursor ions were isolated using MS (quadrupole) and fragmented in an argon filled collision cell (4×10^{-3} mbar). MS/MS data were acquired with the collision energy adjusted in such a way that the majority of the precursor ion was attenuated. Collision energies used were typically between 50 and 100 eV.

2.5. Data interpretation algorithm

The computer algorithm for mass spectrometry data interpretation was developed by using Borland Delphi 7 for Windows (Borland). The proposed algorithm consists of two stages: compositional calculation and in silico fragmentation followed by matching with experimental MS/MS data. The composition of the respective glycoconjugate ions was modelled by using different combinations of monosaccharide and amino acids building blocks, as well as various types of anionization, that is, deprotonation, etc. In silico fragmentation was based on the principle of glycan structure presentation as a 3D array of data, containing information about current building blocks and their mutual linkages. The more detailed description is in preparation and will be published elsewhere.

2.6. Glycan database

Consortium for functional glycomics (CFG): Glycan database has been searched by sending compositional information of the structure, such as the type and the number of monosaccharide building blocks. The list of previously described oligosaccharide structures related to the imported composition was generated as the output, providing information about the sample source, methods of structural elucidation and the corresponding references.[39]

3. Results and discussion

3.1. Automated MALDI-QTOFMS of ALM3 mixture containing glycans and glycosylated amino acids

In the negative ion mode MALDI-QTOFMS of the ALM3 sample around 50 distinct ionic species with

the most intense signals at *m/z* 876.29 and 1038.35 were observed (Fig. 2). A compositional assignment of detected components by a previously developed computer-assisted analysis was applied,[18,19] which implies different combinations of glycan building blocks (dHex, Hex, HexNAc and NeuAc), amino acids (Ser, Thr) and possible sugar modifications such as phosphates (P) and sulfates (S) at various types of anionization, that is, deprotonation and exchange of sodium and potassium versus hydrogen. All ionic species from the mass spectrum expressing relative intensity above 20% have been submitted for calculation.

Within the accepted mass deviation window of 0.15 DA, the composition of approximately 75% ionic species present in the spectrum has been proposed with the mass accuracy in the range of 2–55 ppm (Table 1). According to the compositional analysis 10 molecular ions were proposed to represent glycopeptides, whereas the other represented free oligosaccharides. Molecular ions at *m/z* 873.33, 939.28, 955.29 and 1018.32 were proposed by calculation to represent single amino acid-linked neutral O-glycans such as $[dHexHexNAc_3Thr-H]^-$, $[dHexHex_3HexNAcSer-H]^-$, $[Hex_4HexNAcSer-H]^-$ and $[Hex_3HexNAc_2Ser+Na-2H]^-$, respectively. Five molecular ions, detected at *m/z* 1139.44, 1152.37, 1174.34, 1271.51 and 1293.48 were matching the composition of single amino acid-linked sialylated O-glycans $[NeuAcHex_2HexNAc_2Thr-H]^-$, $[NeuAc_2HexHexNAcSerThr-H]^-$, $[NeuAc_2HexHexNAcSerThr+Na-2H]^-$, $[NeuAcdHexHex_2HexNAc_2Ser-2H]^-$ and $[NeuAcdHexHex_2HexNAc_2Ser+Na-2H]^-$, respectively. The ion at *m/z* 887.22 could be matched to the single amino acid phosphorylated O-glycan $[Hex_3HexNAcThr(P)-H]^-$. Monitoring the ratio between Hex and HexNAc units in the proposed compositions and applying the basic principles of oligosaccharide assembly,[40] the ions detected at *m/z* 1565.56, 1727.61, 1930.67 and 2076.77 were proposed to represent free N-glycans. Composition of these ions obtained by computation was $[NeuAcHex_4HexNAc_3-H]^-$, [Neu-

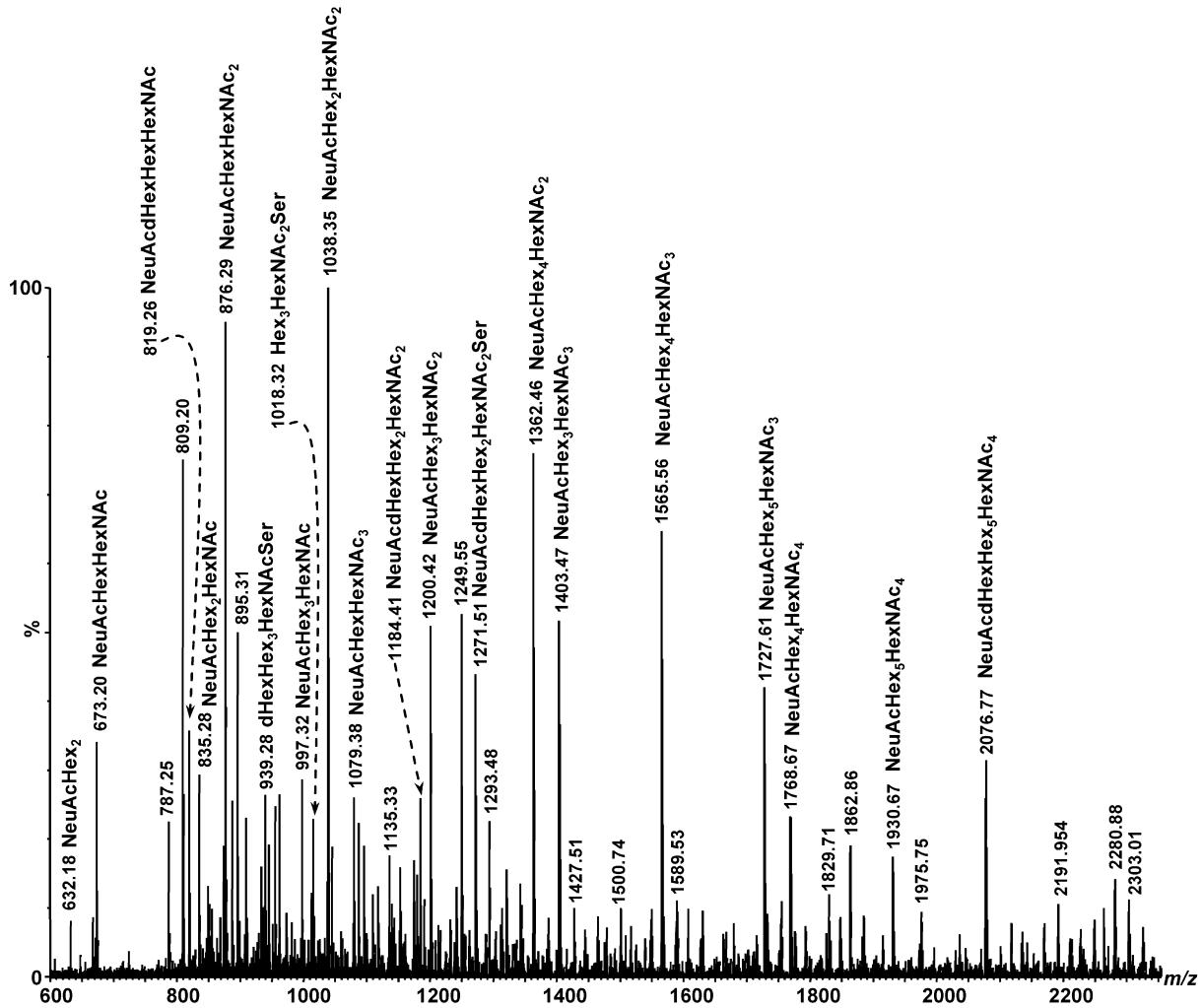

Figure 2. Negative ion mode MALDI-QTOFMS of the fraction M3 obtained from urine of the patient AL after gel permeation chromatography. Peaks are labelled as their monoisotopic *m/z* values.

Table 1. Computer-assisted assignment of major molecular ion species detected in the ALM3 mixture by negative ion MALDI-QTOFMS (Fig. 1)

No	Detected ions			Proposed composition	References[a]
	Ionic species	m/z_{exp}	m/z_{calcd}		
1	$[M-H]^-$	632.18	632.20	$NeuAcHex_2$	41,42
2	$[M+Na-2H]^-$	671.14	671.16	$dHexHexNAc_2(S)$	—
3	$[M-H]^-$	673.20	673.23	NeuAcHexHexNAc	41,42,54,60–65
4	$[M-H]^-$	819.26	819.29	NeuAcdHexHexHexNAc	[b]
5	$[M-H]^-$	835.28	835.28	$NeuAcHex_2HexNAc$	66
6	$[M-H]^-$	873.33	873.35	$dHexHexNAc_3Thr$	—
7	$[M-H]^-$	876.29	876.31	$NeuAcHexHexNAc_2$	52,61
8	$[M-H]^-$	887.22	887.26	$Hex_3HexNAcThr(P)$	—
9	$[M-H]^-$	939.28	939.33	$dHexHex_3HexNAcSer$	—
10	$[M-H]^-$	955.29	955.33	$Hex_4HexNAcSer$	—
11	$[M-H]^-$	997.32	997.34	$NeuAcHex_3HexNAc$	[c]
12	$[M+Na-2H]^-$	1018.32	1018.33	$Hex_3HexNAc_2Ser$	—
13	$[M-H]^-$	1038.35	1038.36	$NeuAcHex_2HexNAc_2$	54,61,67
14	$[M-H]^-$	1079.38	1079.39	$NeuAcHexHexNAc_3$	[c]
15	$[M+Na-2H]^-$	1132.33	1132.29	$Hex_5HexNAc(P)$	—
16	$[M-H]^-$	1139.44	1139.41	$NueAcHex_2HexNAc_2Thr$	—
17	$[M-H]^-$	1143.40	1143.40	$NeuAcdHexHex_3HexNAc$	—
18	$[M-H]^-$	1152.37	1152.41	$NeuAc_2HexHexNAcSerThr$	—
	$[M+Na-2H]^-$	1174.34	1174.39		
19	$[M-H]^-$	1184.41	1184.42	$NeuAcdHexHex_2HexNAc_2$	[c]
20	$[M-H]^-$	1200.42	1200.42	$NeuAcHex_3HexNAc_2$	41,68
21	$[M-H]^-$	1241.45	1241.44	$NeuAcHex_2HexNAc_3$	[c]
22	$[M-H]^-$	1271.51	1271.45	$NeuAcdHexHex_2HexNAc_2Ser$	—
	$[M+Na-2H]^-$	1293.48	1293.43		
23	$[M-H]^-$	1362.46	1362.47	$NeuAcHex_4HexNAc_2$	59,68
24	$[M-H]^-$	1403.47	1403.50	$NeuAcHex_3HexNAc_3$	[c]
25	$[M-H]^-$	1500.47	1500.48	$dHexHex_4HexNAc_3(P)$	—
26	$[M-H]^-$	1565.56	1565.55	$NeuAcHex_4HexNAc_3$	68–70
27	$[M-H]^-$	1727.61	1727.60	$NeuAcHex_5HexNAc_3$	59,68–70
28	$[M-H]^-$	1768.67	1768.63	$NeuAcHec_4HexNAc_4$	[b]
29	$[M-H]^-$	1930.67	1930.68	$NeuAcHex_5HexNAc_4$	43,69,71
30	$[M-H]^-$	2076.77	2076.74	$NeuAcdHexHex_5HexNAc_4$	43,71

[a] References are related to glycoconjugates previously found in *Homo sapiens* urine as free molecular species or as glycans obtained by protein deglycosylation.
[b] Glycoconjugates found in different organs from *Homo sapiens* urogenital system, besides urine.
[c] Glycoconjugates found in *Homo sapiens* from systems other than urogenital.

$AcHex_5HexNAc_3-H]^-$, $[NeuAcHex_5HexNAc_4-H]^-$ and $[NeuAcdHexHex_5HexNAc_4-H]^-$, respectively, where the presence of $Hex_3HexNAc_2$ element in the structure could represent a pentasaccharide core $Man_3GlcNAc_2$, typical for N-glycans. Other glycoforms listed in the table can fit to free oligosaccharides derived either from O-glycans or from truncated N-glycans.

Eleven ions detected in the M3 urine fraction of a CDG patient A.L. and considered as free oligosaccharides arising from glycoproteins were previously found either in the urine of healthy persons and/or patients suffering from different diseases. The urinary trisaccharides $NeuAcHex_2$ and NeuAcHexHexNAc detected at m/z 632.18 and 673.20, respectively, could be correlated to NeuAc(α2–3)Man(β1–4)Glc and NeuAc(α2–6)Man(β1–4)GlcNAc, respectively, already found in the urine of a patient suffering from mannosidosis[41] or to NeuAc(α2–3/6)Gal(β1–4)Glc and NeuAc(α2–3)-Gal(β1–4)GlcNAc, respectively, collected from the normal urine of a male aged 23–25 years,[42] respectively. Similar correlation can be established to singly charged ion detected in the spectrum at m/z 2076.77 (Fig. 2), previously detected in the urine of a healthy male donor as the glycan N-linked to uromodulin and identified by monosaccharide analysis and ^1H NMR as the monosialylated biantennary N-glycan containing core fucose: NeuAc(α2–6)Gal(β1–4)GlcNAc(β1–2)Man(α1–3)-[Gal(β1–4)GlcNAc(β1–2)Man(α1–6)]Man(β1–4)GlcNAc-(β1–4)[Fuc(α1–6)]GlcNAc.[43] References for other structures previously found in the human urine are listed in Table 1.

Thus, according to the MALDI-QTOFMS preliminary analysis of ALM3 sample and the calculation of the composition, most components were considered to represent either free oligosaccharides or O-glycosylated Ser or Thr, in the ratio approximately 4:1. For sequence elucidation of molecular species listed in the table, CID analysis by the negative ion mode MALDI-QTOFMS/MS has been performed.

3.2. Strategy for glycan assignment by fragmentation

Within the development of automated MS/MS data interpretation, the concept of comparison between experimental spectrum and the fragmentation pattern generated from the proposed structure in silico has been probed by several groups.[44–48] MS/MS data contain ions from both glycosidic and internal cross-ring cleavages as well as their mutual combinations resulting in double, sometimes triple, fragmentation. The glycan sequence determination is generally based on glycosidic cleavages, where branching pattern and linkages between monosaccharides must be evaluated from cross-ring fragmentation. Taking into account the importance of these ions for structural characterization of sugar moieties, a computer calculation of all possible elements containing single glycosidic and internal cleavages as well as their mutual combinations, like double glycosidic and A-type cross-ring/glycosidic fragment ions, has been used.

The compositional analysis of fragment ions allows to estimate their potential relation to the parent ion (P.I.) as glycosidic and/or cross-ring cleavages. The inspection of MS/MS data for the presence of diagnostic and unique ions in the spectrum, such as $^{0,2}A_n$ cross-ring fragment ion diagnostic for the HexNAc motif at the reducing end,[19] $^{2,4}A_n$ diagnostic for the branching HexNAc at the reducing end,[19,35] as well as the presence of double glycosidic cleavages 'D' ions responsible for the branching determination of the pentasaccharide core of N-type oligosaccharides[35,49] plays an important role in structural determination.

Taking this into account, as well as biosynthetic rules of glycan assembly[24,40] and the presence of diagnostic ions, fragment ions can be reconstituted into entire potential structural candidates. In case of insufficient or incomplete fragmentation information, certain structural recommendations can still be clearly postulated. However, not all theoretical fragment ions do appear in the spectra, even under optimized CID experimental conditions. Next step of the suggested strategy is to correlate proposed candidates with the previously reported glycan structures which are present in the database[39] or in case of low informative MS/MS data to make a glycan database search for structures fitting by composition and to postulate structural recommendations. In the next step, in silico fragmentation of structural candidates is performed and matched with experimental data to calculate the assignment coverage. Finally, proposed structural candidates are ranked according to the assignment coverage and by the presence of unique and/or diagnostic fragment ions.

3.3. Fragmentation analysis of ionic species observed in ALM3 mixture by MALDI-QTOFMS/MS

Precursor ion at m/z 876.29 assigned to NeuAcHexHexNAc$_2$ (Fig. 2) was submitted to low energy CID tandem MS/MS fragmentation analysis for structural identification (Fig. 3).

B_1 fragment ion at m/z 290.06 indicates the presence of NeuAc in the structure. Diagnostic ring cleavage $^{0,4}A_2$ ion with the loss of CO_2 at m/z 306.08 indicates the attachments of NeuAc to Hex at the linkage position (α2–6).[50,51] Glycosidic cleavage ions B and C at m/z 655.19 and 673.21 state the attachment of HexNAc to NeuAc(α2–6)Hex unit to form trisaccharide. Moreover, compositional analysis of the fragment ion at m/z 572.15 indicates that in case of the tetrasaccharide with one hexose, this ion can only be formed as $^{0,2}A$ ring cleavage of HexNAc unit related to glycosidic fragment ion at m/z 673.21. By further inspection of MS/MS the loss of $\Delta m = 101$ u from the $[M-H]^-$ precursor ion at m/z 775.23 is found, which corresponds to the $^{0,2}A_n$ ion. The presence of this ring cleavage ion indicates the HexNAc unit at the free reducing end of the molecule.[19] On the other hand, the diagnostic ring cleavage ion $^{2,4}A_n$ detected as Δm loss of 161 u from the precursor ion $[M-H]^-$ does not allow branching of the HexNAc at the reducing end, but the extension of only one hydroxyl group at C-3 or C-4 sugar ring position. Thus, taking into account biosynthetic pathways of glycan assembly[24,40] we can propose two potential structural recommendations: HexNAc(1–3)HexNAc followed by the attachment of NeuAc(α2–6)Hex or Hex(1–3)HexNAc followed by the attachment of the NeuAc and the HexNAc to the Hex.

According to the proposed strategy, glycan database search with applied structural recommendations allowed to correlate the precursor ions at m/z 876.29 with two potential candidates summarized in Table 2. NeuAc(α2–6)Gal(1–3/4)GalNAc(α1–3)GalNAc type Core 5 O-glycan (Structure A) was previously found in human urine, but linkage positions and glycans anomeric configurations were not fully specified.[52] Another structural candidate was found in the human haemic system as a type Core 1 O-glycan attached to Glycophorin A and determined by methylation analysis and ^{1}H NMR as GalNAc(β1–4)[NeuAc(α2–3)]Gal(β1–3)GalNAc (Structure B).[53] These two structural candidates provide equal assignment coverage, where the structure type Core 5 assigned to NeuAc(α2–6)Gal(1–3/4)GalNAc(α1–3)GalNAc and previously found in the urine can be considered as the most preferable candidate.[52]

Precursor ion at m/z 1038.35 proposed as NeuAcHex$_2$HexNAc$_2$ (Fig. 2), submitted to fragmentation analysis (Fig. 4), delivered fragment ions at m/z 937.30, 919.29 and 859.27, which can unambiguously be assigned to $^{0,2}A_n$, $^{0,2}A_n$-H_2O and $^{2,4}A_n$-H_2O ring cleavages. Their presence in the spectrum indicates that the reducing end of the molecules consists of HexNAc, where only one carbon group can be further extended by the attachment of other monosaccharides. The loss of HexNAc from the precursor ion $[M-H]^-$ detected at m/z

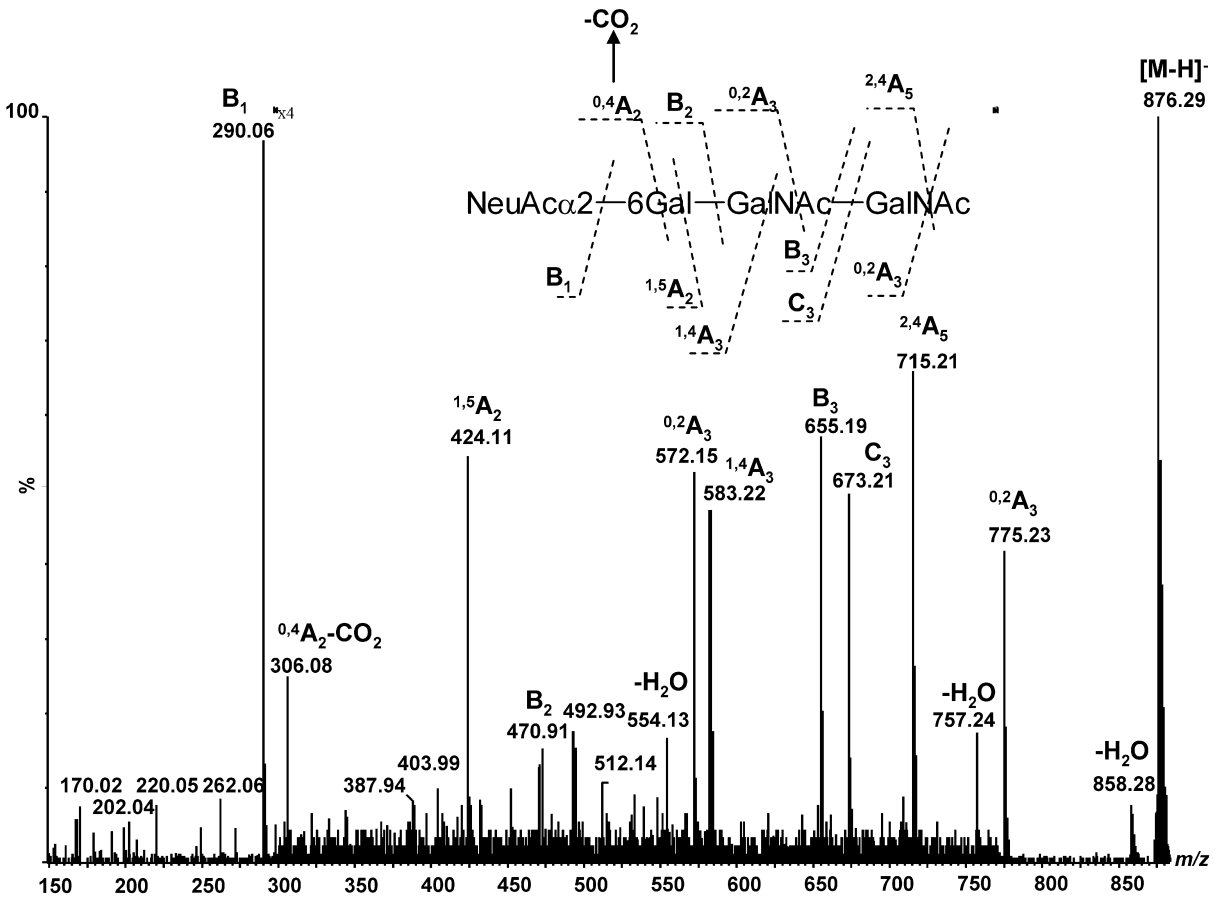

Figure 3. Negative ion mode MALDI-QTOFMS/MS of the precursor ions at *m/z* 876.29 assigned to $NeuAcHexHexNAc_2$. The fragmentation pattern is considered as the most probable according to the fragment ion coverage and the presence of diagnostic ions (inset).

Table 2. Structural candidates for the precursor ions at *m/z* 876.29 assigned to $NeuAcHexHexNAc_2$

Structure	Source[a]
NeuAcα2–6Gal-GalNAc-GalNAc (A)	Urine[52]
GalNAcβ1 → 4 Galβ1—3GalNAc (B); NeuAcα2 → 3	Haemic system[53]

[a] References are related to glycoconjugates previously described.

835.27 can be considered as an evidence that HexNAc is an external element of the entire molecule and assigned to C_n glycosidic fragment. Glycosidic B_1 fragment ion at *m/z* 290.06 shows the presence of sialic acid, whereas B and C type fragments detected at *m/z* 655.21 and 673.20 confirm the NeuAcHexHexNAc increment.

Thus, the search for this composition within human glycans in databases[39] with elucidated structural recommendations allows to correlate this precursor ion with four potential structural candidates, summarized in Table 3. The sialylated diLacNAc N-glycan antennae structure NeuAc(α2–3/6)Gal(β1–4)GlcNAc(β1–3)Gal-(β1–4)GlcNAc (Structure A) was previously discovered in the urine of a 41 year old woman by ^{1}H NMR, methylation analysis and FABMS.[54] Two other linear structures (Structures B and C) were discovered by ^{1}H NMR in the respiratory system (lung) of patients suffering from cystic fibrosis[55] and bronchiectasis,[56,57] and in the intestine of a patient suffering from adenocarcinoma,[58] respectively. The fourth structural candidate with the composition fitted to the precursor ions at *m/z* 1038.35 (Fig. 2) was the synthetic pentasaccharide Gal(β1–4)GlcNAc(β1–4)[NeuAc(α2–3)]Gal(β1–4)GlcNAc (Structure D).[39] Since the assignment coverage of experimental fragment ions provides nearly the same percentage for all structural candidates, the preference can be given to Structure A, according to its origin (previously found in human urine).[54]

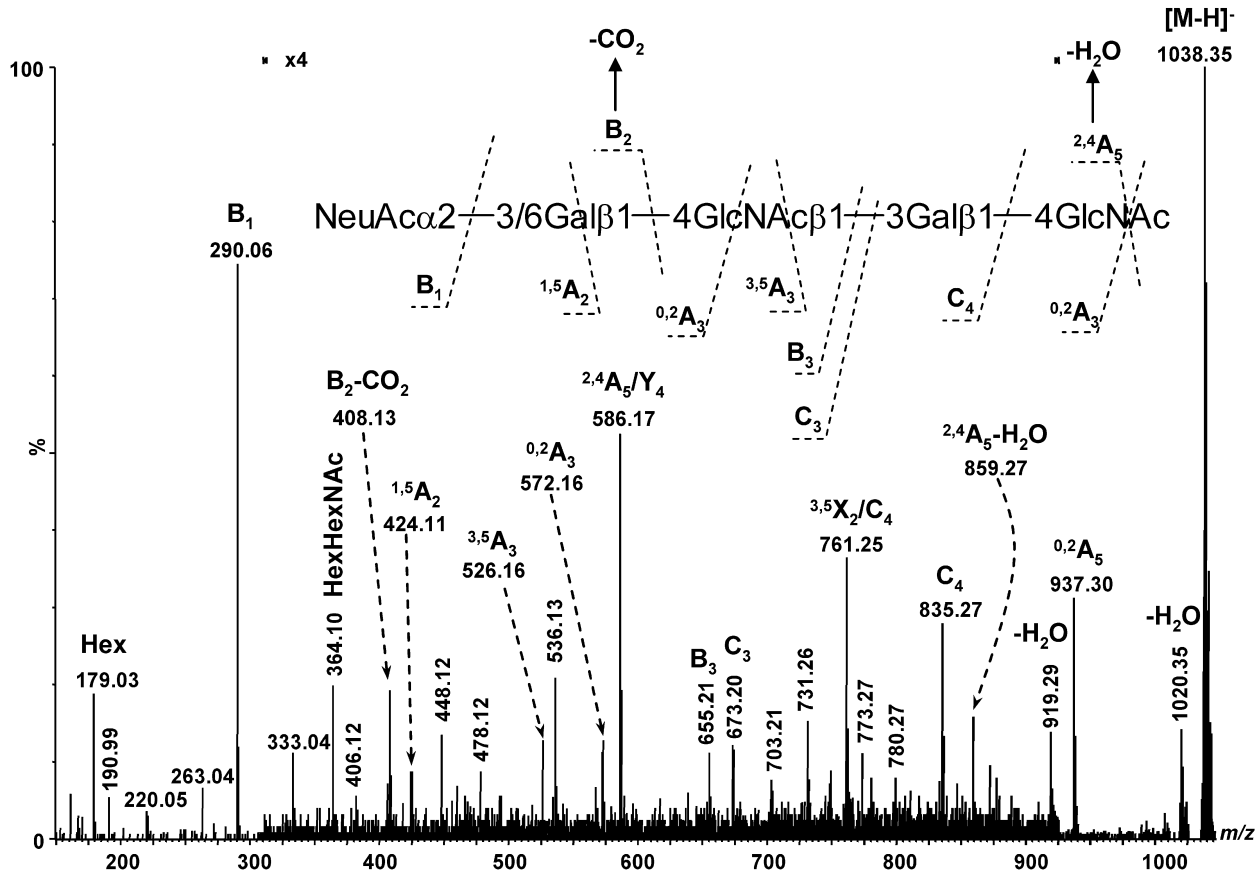

Figure 4. Negative ion mode MALDI-QTOFMS/MS of the precursor ions at *m/z* 1038.35 assigned to $NeuAcHex_2HexNAc_2$. The fragmentation pattern is considered as the most probable according to the fragment ion coverage and the presence of diagnostic ions (inset).

Table 3. Structural candidates for the precursor ions at *m/z* 1038.35 assigned to $NeuAcHex_2HexNAc_2$

Structure	Source[a]
NeuAcα2–3/6Galβ1–4GlcNAcβ1–3Galβ1–4GlcNAc (A)	Urine[54]
NeuAcα2–3/6Galβ1–4GlcNAcβ1–3Galβ1–3GalNAc (B)	Respiratory systems[55]
NeuAcα2–3/6Galβ1–3GlcNAcβ1–3Galβ1–3GalNAc (C)	Digestive system[56,57]
Galβ1—4GlcNAcβ1 (4, 3) Galβ1—4GlcNAc; NeuAcα2 (D)	Synthetic[39]

[a] References are related to glycoconjugates previously described.

According to biosynthetic rules, the precursor ion at *m/z* 1362.46 assigned to $NeuAcHex_4HexNAc_2$ (Fig. 2) could be correlated with both truncated N- and O-glycan chains. Fragmentation pattern performed by CID tandem MS/MS is shown in Figure 5.

As previously discussed, the presence of ring cleavages $^{0,2}A_n$, $^{0,2}A_n$-H_2O and $^{2,4}A_n$ at *m/z* 1261.41, 1243.41 and 1201.39 indicates the HexNAc segment at the reducing end with the structural elongation at only one carbon group of the sugar ring. Glycosidic fragment ions B_1 at *m/z* 290.05 (NeuAc), as well as the loss of HexNAc observed as Y_n and Z_n fragment ions at *m/z* 1071.35 and 1089.39 indicate that NeuAc and HexNAc units are the terminal elements of the molecule. B fragment ion at *m/z* 655.19 (sialylated HexHexNAc) and B and C ions at *m/z* 817.24 and 835.25, respectively, are related to the tetrasaccharide $NeuAcHex_2HexNAc$. Compositional analysis of the fragment ion at *m/z* 545.15 and 730.21 allows to correlate it with Hex_3+60 u and $Hex_3HexNAc(-H_2O)$ + 60 u increments, respectively, which might originate from a combination of glycosidic Y type and cross-ring $^{0,2}X$ and $^{2,4}A$ cleavages, either from Hex or HexNAc. According to biosynthetic considerations, the glycan Hex_3 element can be highly probably hypothesised as a trimannosyl core of an N-glycan.

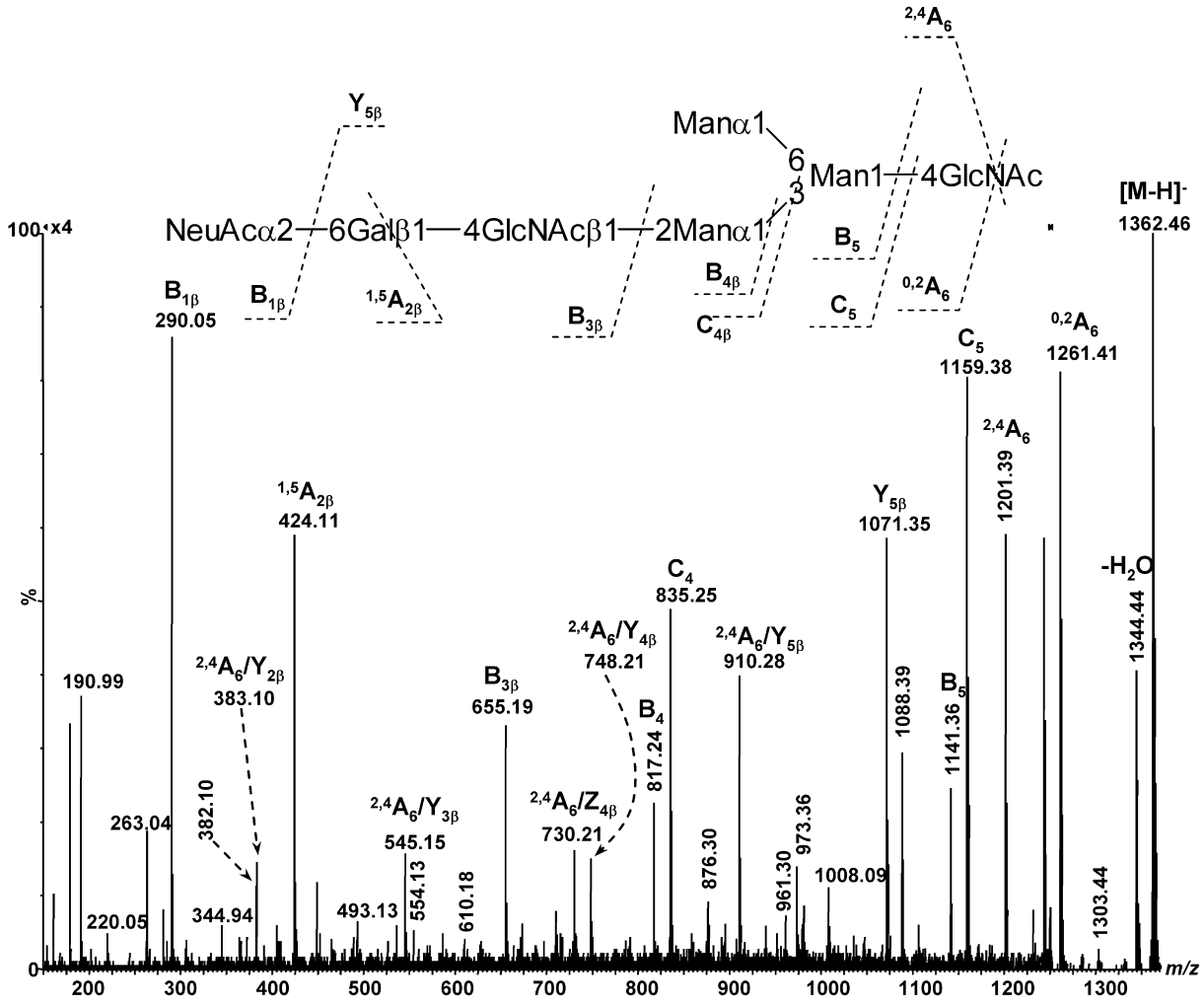

Figure 5. Negative ion mode MALDI-QTOFMS/MS of the precursor ions at *m/z* 1362.46 assigned to $NeuAcHex_2HexNAc_2$. The fragmentation pattern is considered as the most probable according to the fragment ion coverage and the presence of diagnostic ions (inset).

Accordingly, potential structural candidates can be proposed as truncated N-glycans differing in the position of sialylated LacNAc antennae attachment to the core region: NeuAc(α2–3/6)Gal(β1–4)GlcNAc(β1–2)-Man(α1–3)[Man(α1–6)]Man(β1–4)GlcNAc or NeuAc-(α2–3/6)Gal(β1–4)GlcNAc(β1–2)Man(α1–6)[Man(α1–3)]-Man(β1–4)GlcNAc (Table 4). It was previously shown that the Man(α1–3)Man linkage is more labile than the Man(α1–6)Man one, rendering diagnostic $C_{4\beta}$ and 'D' fragment ions.[35] The $C_{4\beta}$ fragment ion at *m/z* 835.25 (Fig. 5) assigned to $NeuAcHex_2HexNAc$ represents a sialylated LacNAc antennae attached to Man(α1–3)Man region of the truncated *N*-glycan core region. Glycan database search revealed that this struc-

Table 4. Structural candidates for the precursor ions at *m/z* 1362.46 assigned to $NeuAcHex_4HexNAc_2$

Structure		Source[a]
Manα1 6 3 Man1β—4GlcNAc NeuAcα2—3/6Galβ1—4GlcNAcβ1—2Manα1	(A)	Urine[59,68,72]
NeuAcα2—3/6Galβ1—4GlcNAcβ1—2Manα1 6 3 Man1β—4GlcNAc Manα1	(B)	Urine[72]

[a] References are related to glycoconjugates previously described.

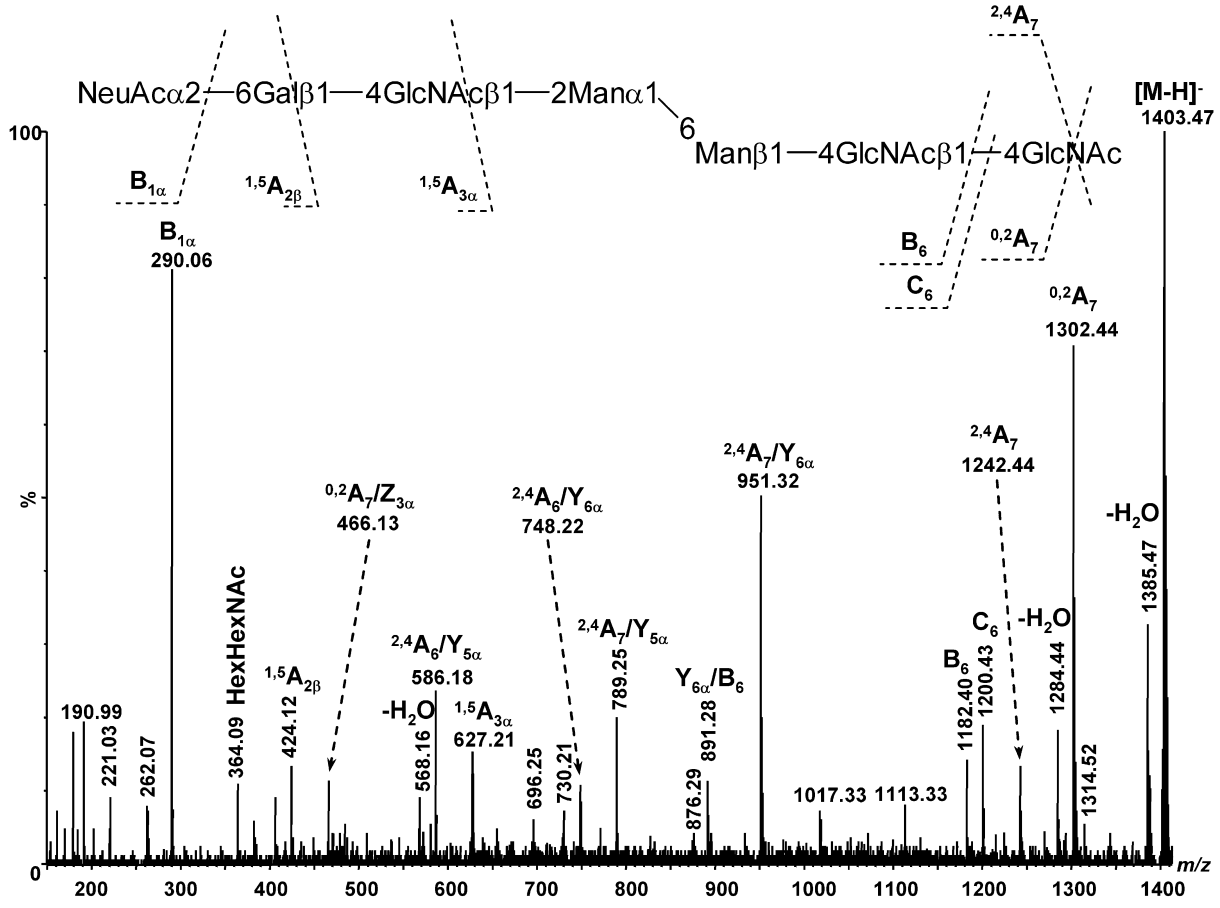

Figure 6. Negative ion mode MALDI-QTOFMS/MS of the precursor ions at *m/z* 1403.47 assigned to $NeuAcHex_2HexNAc_2$. The fragmentation pattern is considered as the most probable according to the fragment ion coverage and the presence of diagnostic ions (inset).

ture was already previously found in the urine of a patient suffering from sialidosis and assigned by monosaccharide analysis and ^1H NMR as NeuAc(α2–6)Gal(β1–4)GlcNAc(β1–2)Man(α1–3)[Man(α1–6)]Man-(β1–4)GlcNAc (Structure A).[59] Thus, this candidates can be considered as the proposed structure for the precursor ion at *m/z* 1362.46. On the other hand, some low intensity fragments ion like *m/z* 493.13 assigned to NeuAcHexNAc and *m/z* 876.30 assigned to NeuAcHexHexNAc$_2$ could not be correlated to the proposed structures. This fact can be indicative for the existence of other isomers related to this precursor ion.

In some other cases, the evidence was less clear, like in the fragmentation pattern of the precursor ion at *m/z* 1403.47 assigned to $NeuAcHex_3HexNAc_3$ (Fig. 6) which does not allow to elucidate the glycan structure explicitly. Few characteristic fragment ions allow, however, to propose recommendations for potential structural candidate in glycan database search.

The presence of $^{0,2}A_n$ and $^{0,2}A_n$-H_2O ring cleavage fragment ions at *m/z* 1302.44 and 1284.44 indicates the position of the HexNAc unit at the free reducing end. $^{2,4}A_n$ cross-ring ion at *m/z* 1242.44 was another key fragmentation determining that the HexNAc element at the reducing end can be further elongated by the attachment to only one hydroxyl group in the sugar ring at the position at C-3 or C-4. Thus applying these considerations, only two structures, corresponding to synthetic oligosaccharides, were found in the glycan database (Table 5).[39] Structure A was the synthetic truncated N-glycan with (α2–6) sialylated LacNAc antennae, whereas the structural candidate B was represented as (α2–3) sialylated $(LacNAc)_3$ N-glycan antennae. In silico fragmentation and further matching with experimental MS/MS data provided the highest assignment coverage of 83% for Structure A, in contrast to 76% for Structure B. In addition, fragment ions at *m/z* 730.21 and 748.22 could only be derived from Structure A and assigned to $^{2,4}A_6/Z_{6\alpha}$ and $^{2,4}A_6/Y_{6\alpha}$, respectively. Thus, NeuAc(α2–6)-Gal(β1–4)GlcNAc(β1–2)Man(α1–6)Man(β1-4)GlcNAc-(β1-4)GlcNAc (Structure A) was considered as the most likely candidate.

Due to the generation of predominantly singly charged ionic species by MALDI-QTOFMS, it was possible to reduce the level of overlapping, like in ESI generated ions, between glycoforms detected in the urine

Table 5. Structural candidates for the precursor ions at *m/z* 1403.47 assigned to $NeuAcHex_3HexNAc_3$

Structure		Source[a]
NeuAcα2—6Galβ1—4GlcNAcβ1—2Manβ1 6 Manβ1—4GlcNAcβ1—4GlcNAc	(A)	Synthetic[39]
NeuAcα2–3Galβ1–4GlcNAcβ1–3Galβ1–4GlcNAcβ1–3Galβ1–4GlcNAc	(B)	Synthetic[39]

[a] References are related to glycoconjugates previously described.

of a CDG patient. The absence of multiply charged fragment ions derived from the precursor ions in CID analysis enhanced the reliability of the elucidated glycan structures, improving significantly the efficacy of the automated compositional analysis and fragmentation pattern interpretation.

A direct computer-assisted compositional assignment is proved to be a potent tool for the determination of glycoconjugates composition in case of free and amino acid-linked oligosaccharides containing sialic acid or phosphates and is highly suitable for high-throughput glycoscreening. Detailed fragmentation patterns of single components from the urine of a CDG patient obtained by MALDI-QTOF CID MS/MS were introduced for glycan database search together with in silico fragment calculation, representing an efficient platform for rapid glycoidentification, or—in the case of lower sequence coverage—to afford appropriate hints for database search. Confirmation of the MALDI-QTOF CID MS/MS approach is obtained by correlation with data obtained by nano-ESI-QTOF CID MS/MS.[18–20] Thus, the ability of MALDI-QTOF instrumentation to provide a comparable set of glycome information from the urine using a minimal amount of sample makes this method especially beneficial for clinical glycomics applications.

References

1. Harvey, D. J. *Mass Spectrom. Rev.* **1999**, *18*, 349–450.
2. Harvey, D. J. *J. Am. Soc. Mass Spectrom.* **2000**, *11*, 900–915.
3. Harvey, D. J. *Proteomics* **2001**, *1*, 311–328.
4. Park, Y.; Lebrilla, C. B. *Mass Spectrom. Rev.* **2005**, *24*, 232–264.
5. Peter-Katalinić, J. *Mass Spectrom. Rev.* **1994**, *13*, 77–90.
6. Zaia, J. *Mass Spectrom. Rev.* **2004**, *23*, 161–227.
7. Keir, G.; Winchester, B. G.; Clayton, P. *Ann. Clin. Biochem.* **1999**, *36*, 20–36.
8. Yarema, K. J.; Bertozzi, C. R. *Genome Biol.* **2001**, *2*, REVIEWS0004.
9. Jaeken, J.; Vanderschueren-Lodeweyckx, M.; Casaer, P.; Snoeck, L.; Corbeel, L.; Eggermont, E.; Eeckels, R. *Pediat. Res.* **1980**, *16*, 179.
10. Jaeken, J.; van Eijk, H. G.; van der, H. C.; Corbeel, L.; Eeckels, R.; Eggermont, E. *Clin. Chim. Acta* **1984**, *144*, 245–247.
11. Jaeken, J. *J. Inherit. Metab. Dis* **2004**, *27*, 423–426.
12. http://www.cdgs.com, 2007.
13. Freeze, H. H. *Glycobiology* **2001**, *11*, 129R–143R.
14. Frösch, M.; Bindila, L.; Zamfir, A.; Peter-Katalinić, J. *Rapid Commun. Mass Spectrom.* **2003**, *17*, 2822–2832.
15. Frösch, M.; Bindila, L. M.; Baykut, G.; Allen, M.; Peter-Katalinić, J.; Zamfir, A. D. *Rapid Commun. Mass Spectrom.* **2004**, *18*, 3084–3092.
16. Linden, H. U.; Klein, R. A.; Egge, H.; Peter-Katalinić, J.; Dabrowski, J.; Schindler, D. *Biol. Chem. Hoppe-Seyler* **1989**, *370*, 661–672.
17. Nahrings, C. Diploma Thesis, University of Bonn, Bonn, Germany, 1994.
18. Vakhrushev, S. Y.; Mormann, M.; Peter-Katalinić, J. *Proteomics* **2006**, *6*, 983–992.
19. Vakhrushev, S. Y.; Zamfir, A.; Peter-Katalinić, J. *J. Am. Soc. Mass Spectrom.* **2004**, *15*, 1863–1868.
20. Zamfir, A.; Vakhrushev, S.; Sterling, A.; Niebel, H. J.; Allen, M.; Peter-Katalinić, J. *Anal. Chem.* **2004**, *76*, 2046–2054.
21. Zamfir, A.; Vukelić, Z.; Bindila, L.; Peter-Katalinić, J.; Almeida, R.; Sterling, A.; Allen, M. *J. Am. Soc. Mass Spectrom.* **2004**, *15*, 1649–1657.
22. Wada, Y.; Azadi, P.; Costello, C. E.; Dell, A.; Dwek, R. A.; Geyer, H.; Geyer, R.; Kakehi, K.; Karlsson, N. G.; Kato, K.; Kawasaki, N.; Khoo, K.-H.; Kim, S.; Kondo, A.; Lattova, E.; Mechref, Y.; Miyoshi, E.; Nakamura, K.; Narimatsu, H.; Novotny, M. V.; Packer, N. H.; Perreault, H.; Peter-Katalinić, J.; Pohlentz, G.; Reinhold, V. N.; Rudd, P. M.; Suzuki, A.; Taniguchi, N. *Glycobiology* **2007**, *17*, 411–422.
23. Domon, B.; Mueller, D. R.; Richter, W. J. *Int. J. Mass Spectrom. Ion Processes* **1990**, *100*, 301–311.
24. Fukuda, M.; Hindsgaul, O. *Molecular and Cellular Glycobiology*; Oxford University Press: New York, 2000, pp 4–33.
25. Butler, M.; Quelhas, D.; Critchley, A. J.; Carchon, H.; Hebestreit, H. F.; Hibbert, R. G.; Vilarinho, L.; Teles, E.; Matthijs, G.; Schollen, E.; Argibay, P.; Harvey, D. J.; Dwek, R. A.; Jaeken, J.; Rudd, P. M. *Glycobiology* **2003**, *13*, 601–622.
26. Chai, W.; Piskarev, V.; Lawson, A. M. *Anal. Chem.* **2001**, *73*, 651–657.
27. Chai, W.; Piskarev, V.; Lawson, A. M. *J. Am. Soc. Mass Spectrom.* **2002**, *13*, 670–679.
28. Harvey, D. J. *J. Mass Spectrom.* **2000**, *35*, 1178–1190.
29. Harvey, D. J. *J. Am. Soc. Mass Spectrom.* **2001**, *12*, 926–937.
30. Mechref, Y.; Novotny, M. V. *Chem. Rev.* **2002**, *102*, 321–369.
31. Pfenninger, A.; Karas, M.; Finke, B.; Stahl, B. *J. Am. Soc. Mass Spectrom.* **2002**, *13*, 1331–1340.
32. Que, A. H.; Novotny, M. V. *Anal. Bioanal. Chem.* **2003**, *375*, 599–608.
33. Quemener, B.; Cabrera Pino, J. C.; Ralet, M. C.; Bonnin, E.; Thibault, J. F. *J. Mass Spectrom.* **2003**, *38*, 641–648.
34. Robbe, C.; Capon, C.; Coddeville, B.; Michalski, J. C. *Rapid Commun. Mass Spectrom.* **2004**, *18*, 412–420.

35. Šagi, D.; Peter-Katalinić, J.; Conradt, H. S.; Nimtz, M. *J. Am. Soc. Mass Spectrom.* **2002**, *13*, 1138–1148.
36. de Hoffmann, E.; Stroobant, V. *Mass Spectrometry. Principles and Applications*, 2nd ed.; John Wiley & Sons, Ltd: Chichester, West Sussex, England, 2002.
37. Bindila, L.; Froesch, M.; Lion, N.; Vukelić, Ž.; Rossier, J. S.; Girault, H. H.; Peter-Katalinić, J.; Zamfir, A. D. *Rapid Commun. Mass Spectrom.* **2004**, *18*, 2913–2920.
38. Domon, B.; Costello, C. E. *Glycoconjugate J.* **1988**, *5*, 397–409.
39. http://www.functionalglycomics.org, 2007.
40. Varki, A.; Cummings, R.; Esko, J.; Freeze, H.; Hart, G.; Marth, J. *Essentials of Glycobiology*; Cold Spring Harbor Laboratory Press: New York, 1999, pp 85–115.
41. Van Pelt, J.; Dorland, L.; Duran, M.; Hokke, C. H.; Kamerling, J. P.; Vliegenthart, J. F. *J. Biol. Chem.* **1990**, *265*, 19685–19689.
42. Parkkinen, J.; Finne, J. *Eur. J. Biochem.* **1983**, *136*, 355–361.
43. Hard, K.; Van Zadelhoff, G.; Moonen, P.; Kamerling, J. P.; Vliegenthart, F. G. *Eur. J. Biochem.* **1992**, *209*, 895–915.
44. Cooper, C. A.; Joshi, H. J.; Harrison, M. J.; Wilkins, M. R.; Packer, N. H. *Nucleic Acids Res.* **2003**, *31*, 511–513.
45. Joshi, H. J.; Harrison, M. J.; Schulz, B. L.; Cooper, C. A.; Packer, N. H.; Karlsson, N. G. *Proteomics* **2004**, *4*, 1650–1664.
46. Lohmann, K. K.; von der Lieth, C. W. *Proteomics* **2003**, *3*, 2028–2035.
47. Lohmann, K. K.; von der Lieth, C. W. *Glycobiology* **2003**, *13*, 846.
48. Tang, H.; Mechref, Y.; Novotny, M. V. *Bioinformatics* **2005**, *21*, i431–i439.
49. Egge, H.; Peter-Katalinić, J. *Mass Spectrom. Rev.* **1987**, *6*, 331–393.
50. Meisen, I.; Peter-Katalinić, J.; Müthing, J. *Anal. Chem.* **2003**, *75*, 5719–5725.
51. Wheeler, S. F.; Harvey, D. J. *Anal. Chem.* **2000**, *72*, 5027–5039.
52. Escribano, J.; Lopex-Otin, C.; Hjerpe, A.; Grubb, A.; Mendez, E. *FEBS Lett.* **1990**, *266*, 167–170.
53. Herkt, F.; Parente, J. P.; Leroy, Y.; Fournet, B.; Blanchard, D.; Cartron, J. P.; Vanhalbeek, H.; Vliegenthart, J. F. G. *Eur. J. Biochem.* **1985**, *146*, 125–129.
54. Irie, F.; Murakoshi, H.; Suzuki, T.; Suzuki, Y.; Kon, K.; Ando, S.; Yoshida, K.; Hirabayashi, Y. *Glycoconjugate J.* **1995**, *12*, 290–297.
55. Breg, J.; Van Halbeek, H.; Vliegenthart, J. F. G.; Lamblin, G.; Houvenaghel, M. C.; Roussel, P. *Eur. J. Biochem.* **1987**, *168*, 57–68.
56. Van Halbeek, H.; Breg, J.; Vliegenthart, J. F.; Klein, A.; Lamblin, G.; Roussel, P. *Eur. J. Biochem.* **1988**, *177*, 443–460.
57. Van Halbeek, H.; Strang, A. M.; Lhermitte, M.; Rahmoune, H.; Lamblin, G.; Roussel, P. *Glycobiology* **1994**, *4*, 203–219.
58. Capon, C.; Laboisse, C. L.; Wieruszeski, J. M.; Maoret, J. J.; Augeron, C.; Fournet, B. *J. Biol. Chem.* **1992**, *267*, 19248–19257.
59. Van Pelt, J.; Kamerling, J. P.; Bakker, H. D.; Vliegenthart, J. F. *J. Inherit. Metab. Dis.* **1991**, *14*, 730–740.
60. Amano, J.; Nishimura, R.; Mochizuki, M.; Kobata, A. *J. Biol. Chem.* **1988**, *263*, 1157–1165.
61. Bhavanandan, V. P.; Zhu, Q.; Yamakami, K.; Dilulio, N. A.; Nair, S.; Capon, C.; Lemoine, J.; Fournet, B. *Glycoconjugate J.* **1998**, *15*, 37–49.
62. Elliott, M.; Kardana, A.; Lustbader, J.; Cole, L. *Endocrine* **1997**, *7*, 15–92.
63. Gadroy, P.; Stridsberg, M.; Capon, C.; Michalski, J. C.; Strub, J. M.; Van, D. A.; Aunis, D.; Metz-Boutigue, M. H. *J. Biol. Chem.* **1998**, *273*, 34087–34097.
64. Garver, F. A.; Chang, L. S.; Kiefer, C. R.; Mendicino, J.; Chandrasekaran, E. V.; Isobe, T.; Osserman, E. F. *Eur. J. Biochem.* **1981**, *115*, 643–652.
65. Van Pelt, J.; Van Bilsen, D. G.; Kamerling, J. P.; Vliegenthart, J. F. *Eur. J. Biochem.* **1988**, *174*, 183–187.
66. Pollitt, R. J.; Pretty, K. M. *Biochem. J.* **1974**, *141*, 141–146.
67. Amano, J.; Nishimura, R.; Sato, S.; Kobata, A. *Glycobiology* **1990**, *1*, 45–50.
68. Nakamura, Y.; Takahashi, Y.; Yamaguchi, S.; Omiya, S.; Orii, T.; Yara, A.; Gushiken, M. *Tohoku J. Exp. Med.* **1992**, *166*, 407–415.
69. de Beer, T.; van Zuylen, C. W.; Hard, K.; Boelens, R.; Kaptein, R.; Kamerling, J. P.; Vliegenthart, J. F. *FEBS Lett.* **1994**, *348*, 1–6.
70. Weisshaar, G.; Hiyama, J.; Renwick, A. G. *Glycobiology* **1991**, *1*, 393–404.
71. Nakano, Y.; Noda, K.; Endo, T.; Kobata, A.; Tomita, M. *Arch. Biochem. Biophys.* **1994**, *311*, 117–126.
72. Kuriyama, M.; Ariga, T.; Ando, S.; Suzuki, M.; Yamada, T.; Miyatake, T.; Igata, A. *J. Biochem.* **1985**, *98*, 1049–1054.